Coumarin Derivatives Exert Anti-Lung Cancer Activity by Inhibition of Epithelial–Mesenchymal Transition and Migration in A549 Cells

Rodrigo Santos Aquino de Araújo, Julianderson de Oliveira dos Santos Carmo, Simone Lara de Omena Silva, Camila Radelley Azevedo Costa da Silva, Tayhana Priscila Medeiros Souza, Natália Barbosa De Mélo, Jean-Jacques Bourguignon, Martine Schmitt, Thiago Mendonça De Aquino, Renato Santos Rodarte, et al.

Coumarin derivatives exert anti-lung cancer activity by inhibition of epithelial-mesenchymal transition and migration in A549 cells

Rodrigo Santos Aquino de Araújo[a,c], Julianderson de Oliveira dos Santos Carmo[b], Simone Lara de Omena Silva[b], Camila Radelley Azevedo Costa da Silva[b], Tayhana Priscila Medeiros Souza[b], Jean-Jacques Bourguignon[c], Martine Schmitt[c], Thiago Mendonça de Aquino[d], Renato Santos Rodarte[b], José Maria Barbosa Filho[e], Emiliano Barreto[b,*,#], Francisco Jaime Bezerra Mendonça Junior[a,e,*,#],

[a] *Department of Biological Sciences, State University of Paraiba, Laboratory of Synthesis and Drug Delivery, João Pessoa, PB, Brazil*

[b] *Institute of Biological and Health Sciences, Federal University of Alagoas, 57072-900, Maceió-Brazil*

[C] *Laboratoire d'Innovation thérapeutique, UMR 7200, Labex Medalis, CNRS, Université de Strasbourg, Faculté de Pharmacie, 74 route du Rhin, BP 60024, 67401 Illkirch, France*

[d] *Research Group on Therapeutic Strategies – GPET, Institute of Chemistry and Biotechnology, Federal University of Alagoas, Maceió, Brazil*

[e] *Post-graduate Program in Natural and Synthetic Bioactive Products, Federal University of Paraíba, 58051-900, João Pessoa, PB, Brazil.*

ABSTRACT: A series of coumarin derivatives and isosteres were synthesized from the reaction of triflic intermediates with phenylboronic acids, terminal alkynes and organozinc compounds, through palladium-catalyzed cross-coupling reactions. The *in vitro* cytotoxic effect of the compounds was evaluated against two non-small cell lung carcinoma (NSCLC) cell lines (A-549 and H2170 (human lung adenocarcinoma cells)) and normal cell line (fibroblast healthy NIH-3T3) using cisplatin (2.6 μM) as reference drug. Additionally, the effects of the most promising coumarin derivative (**9f**) in reversing the epithelial-to-mesenchymal transition (EMT) in IL-1β-stimulated A549 cells, and in inhibiting the EMT-associated migratory ability in A549 cells were also evaluated. Compound **9f** had the greatest cytotoxic effect (CC_{50} = 7.1 ± 0.8 and 3.3 ± 0.5 μM, respectively against A549 and H2170 cells) and CC_{50} value of 25.8 μM for NIH-3T3 cells. Compound **9f** inhibited the IL-1β-induced EMT in epithelial cells by inhibiting the F-actin reorganization, attenuating changes in the actin cytoskeleton reorganization and by downregulating of vimentin in A549 cells stimulated by IL-1β. Treatment of A549 cells with **9f** at 7 μM for 24 h significantly reduced migration of IL-1β-stimulated cells, phenomenon confirmed by qualitative assessment of the wound closure. Taken together, our finding suggest that coumarin derivatives, especially compound **9f** may become a promising candidate for lung cancer therapy, especially in lung cancer promoted by non-small cell lung carcinoma (NSCLC) cell lines.

Keywords: anticancer activity, lung cancer, non-small-cell lung cancer, epithelial-mesenchymal transition, methastasis, coumarin derivative.

[#] These authors contributed equally to this work.

*Corresponding authors: e-mail: emilianobarreto@icbs.ufal.br (E. Barreto); franciscojbmendonca@yahoo.com.br (F.J.B. Mendonça-Junior)

1. Introduction

Cancer is characterized by cells with uncontrolled division, genome heterogeneity, and invasiveness to other tissues via blood or lymph nodes. According to the World Health Organization (WHO) reports, almost 9 million cancer-related deaths annually occur [1]. Among cancers, the lung cancer is one of the most common type, with a mortality rate of around 18.4% according to GLOBOCAN report [2].

Cancer metastasis is defined as the formation of new tumors in tissues away from the primary site, account for a vast majority of morbidity and mortality of patients and is associated with about 90% of all cancer-associated deaths [3,4]. In the past decade, an increasing number of studies have provided strong evidence to proposed that epithelial-mesenchymal transition (EMT) — a known cellular program allowing polarized cells to shift to a mesenchymal phenotype with increased cellular motility [5] — has a central role in cancer progression and metastatic dissemination [6-8]. For this reason, the EMT has become as a target of interest for anticancer therapy [9, 10].

Furthermore, cancer therapy is complex due mainly to drug-resistance, which leads to less effectiveness of the anticancer agents. Therefore, the discovery and development of new chemotherapeutic agents with greater efficacy is very urgent need.

Coumarins are a class of secondary metabolites chemically characterized by the fusion of a benzene with an α-pirone ring [11]. Their pharmacological applications are widely described [12-17], highlighting its applications in the treatment of several human cancer and in the inhibition of cell growth of several cancer cell lines [18-27], including lung cancer [21, 28-37]. Its low toxicities [38, 39], associated with its potential to inhibit several proteins associated with lung cancer (tyrosine kinase, telomerase, NF-κB, ERK1/2, EGFR, STAT proteins, HSP 90, PI3K, Bax, among others) [24, 26, 28], makes them as promising prototypes for the development of new anti-lung cancer drugs.

In view of the above, the aim of this study was to synthesize a series of coumarins derivatives obtained through palladium-catalyzed cross-coupling reactions (PCCCR), and evaluate their cytotoxic effects *in vitro* in two non-small two cell lung carcinoma (NSCLC) cell lines (A549 and H2170). Additionally, were investigated the potential of the most promising coumarin derivative (**6f**) in reversing the epithelial-to-mesenchymal transition (EMT) in IL-1β-stimulated A549 cells, and in inhibiting the EMT-associated migratory ability in A549 cells.

2. Materials and Methods

2.1. Compounds (synthetic coumarins)

Compounds **1d** [40], **3** [41], **5b** [42], **6** [43], **8a** [44], **8d** [45], **9a** [44], **9b** and **9c** [46], **9d** [44], **9g** [47], **10** [43], **12a** [48], **13a** [49] and **17** [50] were synthesized and structure of these compounds has been confirmed by comparison with NMR spectral data from the literature.

All other coumarin derivatives: triflic intermediates (**4, 5a, 5b, 6**); Suzuki-Miyaura adducts (**7**, **8a-g**, **9a-f**); Sonogashira adducts **11**, **12a-c**, **13 a-c**); Negishi adducts (**14** and **15**); and alkyl coumarin derivatives obtained by catalytic hydrogenation (**16** and **17**) were prepared according to the synthetic procedures described in the supplementary material.

2.2. Biological Assays

2.2.1. Cell line and cell culture

A549, H2170 and normal mouse fibroblast (NIH-3T3) cell lines were obtained from the Rio de Janeiro Cell Bank (BCRJ). A549 and NIH-3T3 cells were maintained in Dulbecco's Modified Eagle Medium (DMEM), while H2170 cell line was maintained in Roswell Park Memorial Institute (RPMI)-1640. The culture media were supplemented with 10% fetal bovine serum (FBS), 2 mM L-glutamine, 40 µg/mL gentamicin. All cells were cultured in a humidified atmosphere contained 5% CO_2 incubator

84 at 37 °C. For experiments, cells were grown to 90% confluence. All experiments were conducted using
85 cells with passage numbers less than 10.

86 **2.2.2. Cell viability assay and treatment**

87 The effect of coumarin derivatives on cell viability was evaluated by the MTT assay at a single
88 dose according to NCI testing protocol or at different concentrations for IC_{50} determination [51].
89 Coumarin derivatives were dissolved in dimethyl sulfoxide (DMSO) and then diluted with DMEM.
90 Briefly, cells were plated in 96-well plates (2×10^4/well) and each coumarin derivatives at 12 μM were
91 added to the culture medium and the cell cultures were continued for 24 h. Cisplatin (2.6 μM) was
92 used as a reference drug. Thereafter, the medium was replaced with fresh DMEM containing 5 mg/mL
93 MTT. Following an incubation period (4 h) in a humidified CO_2 incubator at 37 °C and 5% CO_2, the
94 supernatant was removed and dimethyl sulfoxide solution (DMSO, 150 mL/well) was added to each
95 cultured plate. After incubation at room temperature for 15 min, the absorbance of the solubilized MTT
96 formazan product was spectrophotometrically measured at 540 nm. Three individual wells were
97 assayed for each treatment and the percentage viability relative to the control sample was determined
98 as (absorbance of treated cells/absorbance of untreated cells)×100%. Only the compound which
99 reduced the viability by half the value of control cells progressed to the full 5-dose assay with the
100 H2170 cell lines. The concentration of **9f** compound that reduced the viable cell number by 50% (CC_{50})
101 was determined using a non-linear regression approach and the mean value of CC_{50} for each cell type
102 was calculated from triplicate.

103 **2.2.3. Epithelial-to-mesenchymal transition (EMT) induction and coumarin derivatives**
104 **treatment**

105 For induction of EMT process, A549 cells (1×10^5 per well) were seeded in 24-well culture
106 plates and treated with 1 ng/ml IL-1β (Peprotech, NJ, USA) for 24 h. In the unstimulated cells DMEM
107 medium was added. Then, the morphological alteration of cells was observed under a microscope. This

protocol for EMT induction is as reported in previous literature [52]. To evaluate the effects of coumarin derivative with respect to EMT induced by IL-1β, cells were pretreated with compound **9f** at 7 μM, being this treatment also maintained during stimulation with IL-1β for 24 h.

2.2.4. Immunofluorescence staining

After 24 h, cells were fixed for 15 minutes at 4°C with 4% paraformaldehyde in PBS. Cells were permeabilized with 0.1% Triton X-100, washed with PBS. Next, cells were incubated with FITC-conjugated phalloidin (1:100) for 2 h at room temperature, and then rinsed several times with PBS. Following an additional wash step with PBS, cells were stained with 10 μg/ml DAPI at room temperature for 10 min for the visualization of cell nuclei. Cell morphology was determined using an inverted epifluorescence microscope (Nikon Eclipse 50i).

In another set of experiment, the analysis for vimentin, a well-recognized marker for its selective expression and specific role in mesenchymal state, was performed. After treatment, cells were fixed, permeabilized and washed as described above. Next, the slides were incubated with an anti-vimentin antibody (1:100) at 4 °C overnight. The next day, the slides were incubated with secondary antibody goat anti-rabbit-FITC (1:100) dilutions at room temperature for 1 h. Lastly, cells were stained with DAPI (Invitrogen; Thermo Fisher Scientific, Inc.) and washed with PBS. Stained cells were analyzed by a flow cytometer (FACSCanto II, Becton Dickinson, San Jose, CA) accompanied with the BD FACSDIVA™ software for data analysis. The cell-associated fluorescence of 5,000 cells per sample was measured as mean fluorescence intensity (MFI) in the FL1 channel. The MFI values were corrected for unspecific staining by substracting the fluorescence of cells unstained (negative control).

2.2.5. *In vitro* scratch wound healing assay

To evaluate the effect of **9f** on epithelial motility, we performed the scratch assay as described by Cardoso and coworkers [53]. Cells were maintained in 24 well plates until they reached 90%

confluency. Thereafter, a vertical stripe on the cell monolayer was made using a sterile pipette (200 µl) tip. The wells were washed with PBS to remove dead cells and debris, and then **9f** was added at concentration of 7 µM. As a control, the cells were treated with cell culture medium. Photographs were captured by a digital camera connected to inverted microscope (Olympus IX70) at 0 and 24 h after scratch. The migration gap area of the cells was measured by ImageJ software (https://imagej.nih.gov/ij/; Center for Information Technology, National Institute of Health, Bethesda, MA, USA). Each measurement was repeated three times.

2.2.6. Statistical analysis

Data were expressed as mean ± standard deviation (S.D.). The statistical analysis involving two groups was done using Student's t-test. Analysis of variance followed by the Tukey's test were used to compare three or more groups. Values of $p < 0.05$ were considered as indicative of significance.

3. Results and Discussion

3.1. Chemistry

The synthesis of the coumarin core can be performed by different synthetic methodologies, among which the most common are Pechmann, Wittig, Knoevenagel and Perkin reactions [11]. Cross-coupling reactions catalyzed by transition metals, like the Suzuki-Miyaura, Negishi [54] and Sonogashira [55] reactions, have become powerful alternatives to the formation of carbon-carbon bonds [56, 57] and allowed the introduction of various substituents in all positions of the basic nucleus, leading to analogous, homologous or libraries of compounds [58].

The preparation of target compounds (coumarins, quinolones and chromen-4-ones) involved the formation of triflic methanesulfonate derivatives as key intermediates **4**, **5a-b** and **6**, thanks to the cross coupling reactions. 6- and 7–hydroxycoumarin **2a-b** and 6-hydroxyquinolone **1a** are commercially available, and 3-hydroxy-chromen-4-one **3** was synthesized following a reported

preparation [41]. Attemps to prepare 6-OTf quinolone from **1a** and triflic anhydride, resulted exclusively in the formation of the 2,6 di-triflic adduct **1b**. Therefore, our efforts focused on the preparation of N-Me quinolone **1c**. However, N-alkylation of quinolone **1a** needed a first transient protection of the phenol by an acetyl group (compounds **1d-e**) according to scheme 1.

Scheme 1. Synthesis of 1-methyl-6-hydroxy-quinol-2-one (**2c**).

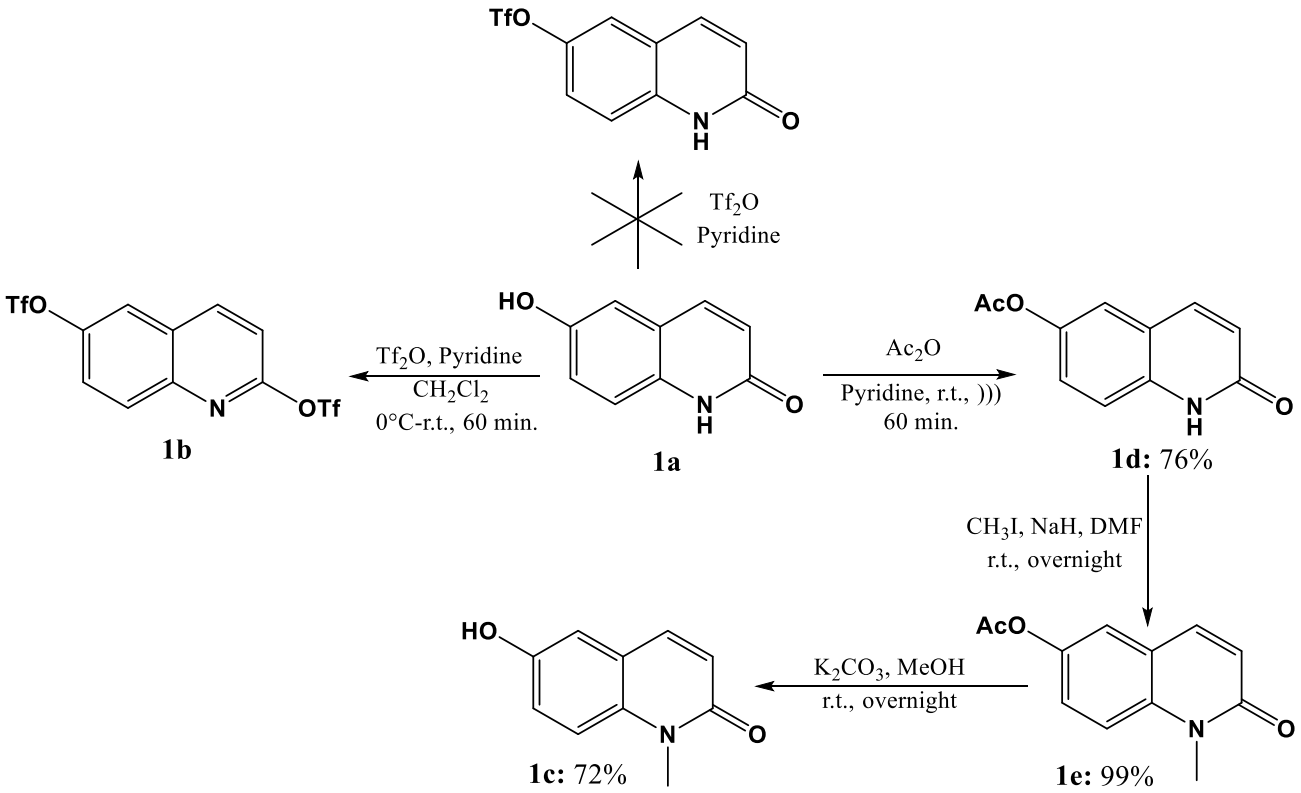

Reaction of the respective hydroxyl cores (cpds **1c**, **2a-b** and **3**) with triflic anhydride in presence of pyridine afforded the corresponding triflic intermediates **4, 5a-b** and **6** in high yields (≥ 75%), as illustrated in scheme 2.

Scheme 2. Synthesis of the triflic intermediates **4**, **5a-b**, **6**.

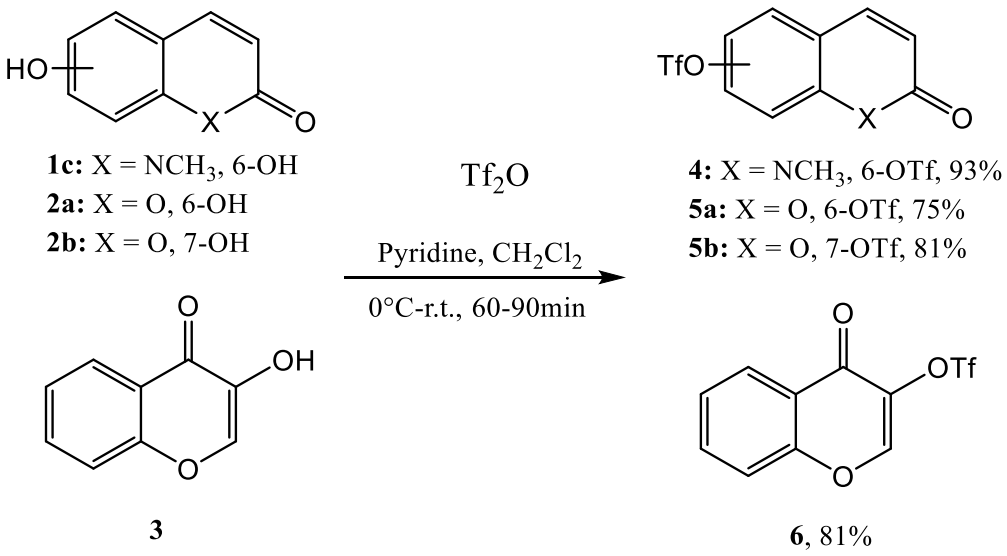

164

165 With triflic intermediates **4**, **5a-b** and 6 in hand, our attention next turn to the Suzuki-Miyaura
166 cross coupling reaction. Reaction with various boronic acids enable preparation of a small library of
167 6- and 7-substituted coumarins (cpds **8a-f**, **9a-g**). The use of a catalytic amount of
168 tetrakis(triphenylphosphine) palladium(0) (5.0 mol%) in presence of $NaHCO_3$ as base, led efficiently
169 to the target compounds (see table 1). However, for the introduction of a pyridin moiety in the
170 coumarin structure, K_3PO_4 was preferred over $NaHCO_3$ (table 1, cpds **8d** and **9g**). For these 2 cpds,
171 the reaction was performed in Toluene/EtOH/H_2O and yielded the expected compounds **8d** and **9g** in
172 74 % and 82 % yields respectively. Starting from the OTf-flavone derivative **6**, the use of $Pd(OAc)_2$
173 (5.0 mol%) in presence of KF furnished **10** in moderate yield (50%) (Scheme 3).

174 **Scheme 3**. Palladium-catalyzed cross-coupling reactions to synthesized coumarin, quinolones and
175 chromen-4-one derivatives.

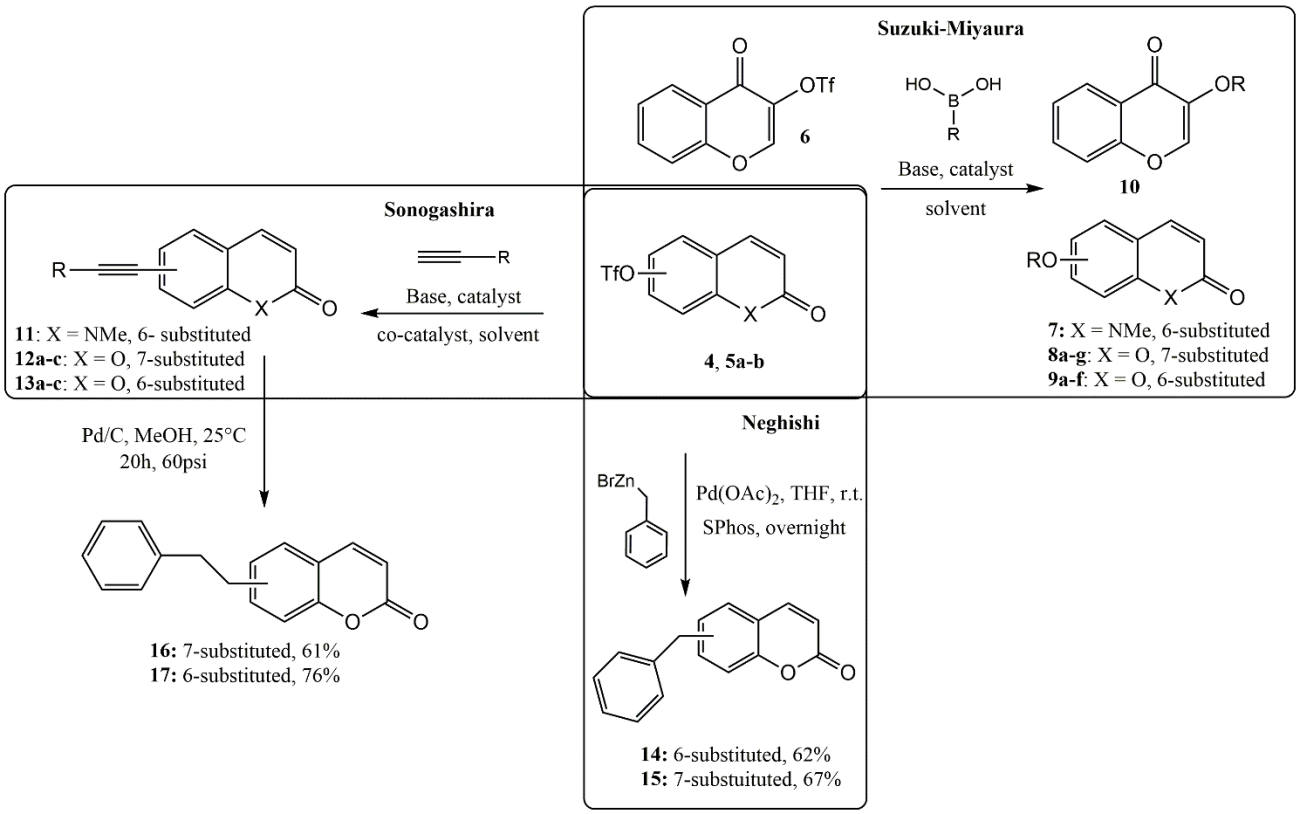

176

177 **Table 1.** Preparation of compounds **7**, **8a-g**, **9a-f** and **10** through Suzuki-Miyaura conditions.

Cpd	X	R	Base	Catalyst. (5.0 mol%)	Solvent	Yield (%)
8a	O	7-(4-OCH_3)-Ph	$NaHCO_3$	$Pd(PPh_3)_4$	MeOH	71
8b	O	7-(2-OCH_3)-Ph	$NaHCO_3$	$Pd(PPh_3)_4$	MeOH	84
8c	O	7-(2-Cl)-Ph	$NaHCO_3$	$Pd(PPh_3)_4$	MeOH	71
8d	O	7-(Pyridin-4-yl)	K_3PO_4	$Pd(PPh_3)_4$	Toluene/EtOH/H_2O (4:1:1)	74
8e	O	7-(4-CF_3)-Ph	$NaHCO_3$	$Pd(PPh_3)_4$	MeOH	78
8f	O	7-(3,4-Cl)-Ph	$NaHCO_3$	$Pd(PPh_3)_4$	MeOH	59
9a	O	6-(4-OCH_3)-Ph	$NaHCO_3$	$Pd(PPh_3)_4$	MeOH	73
9b	O	6-(3-OCH_3)-Ph	$NaHCO_3$	$Pd(PPh_3)_4$	MeOH	71
9c	O	6-(2-OCH_3)-Ph	$NaHCO_3$	$Pd(PPh_3)_4$	MeOH	76

9d	O	6-(4-Cl)-Ph	$NaHCO_3$	$Pd(PPh_3)_4$	MeOH	45
9e	O	6-(2-Cl)-Ph	$NaHCO_3$	$Pd(PPh_3)_4$	MeOH	71
9f	O	6-(3,4-Cl)-Ph	$NaHCO_3$	$Pd(PPh_3)_4$	MeOH	68
9g	O	6-(Pyridin-4-yl)	K_3PO_4	$Pd(PPh_3)_4$	Toluene/EtOH/H_2O (4:1:1)	82
7	NCH_3	6-(4-OCH_3)-Ph	$NaHCO_3$	$Pd(PPh_3)_4$	MeOH	81
10	-	3-(4-OMe)-Ph	KF	$Pd(OAc)_2$	MeOH	50

Sonogashira reaction with different terminal alkynes resulted in 7 compounds (Table 2).

Table 2. Preparation of compounds **11**, **12a-c**, **13a-c** through Sonogashira cross-coupling reaction in CH_3CN.

Cpd	X	R	Base	Ligand/Catalyst	Additive	Yield %
12a	O	Ph	Et_3N	$Pd(PPh_3)_2Cl_2$	CuI	75
12b	O	CH_2OCH_2Ph	Et_3N	$Pd(PPh_3)_2Cl_2$	CuI	38
12c	O	CH_2OH	K_2CO_3	S-Phos/$Pd(OAc)_2$	TBAI	75
13a	O	Ph	K_2CO_3	S-Phos/$Pd(OAc)_2$	TBAI	78
13b	O	$(CH_2)_3Ph$	K_2CO_3	S-Phos/$Pd(OAc)_2$	TBAI	76
13c	O	CH_2OH	K_2CO_3	S-Phos/$Pd(OAc)_2$	TBAI	72
11	NCH_3	Ph	K_2CO_3	S-Phos/$Pd(OAc)_2$	TBAI	78

Palladium-catalyzed Sonogashira cross-coupling is a widely used method to synthesize functional molecules containing an alkyne unit. Traditional Sonogashira coupling with $Pd(PPh_3)_2Cl_2$ (3.0 mol %) and Et_3N typically requires the use of a Cu(I) halide salt as a cocatalyst to have high reaction productivity. So, starting from coumarin **5b** and under these conditions, the phenyl acetylene moiety was introduced under microwave irradiation in 75% yield (cpd **12a**). However, with OBn

propargylalcohol, same conditons yielded **12b** in only 38% yield. Recently, Chorley et al. highlighted the efficacy of $Pd(OAc)_2$ and 2-dicyclohexylphosphino-2′,6′-dimethoxybiphenyl (SPhos) as effective catalytic system for the Sonogashira cross coupling reaction [59]. In addition, the presence of tetrabutylammonium iodide (TBAI) as additive increased the yield of the reaction [59]. Under these conditions and without protection of propargylic alcohol, we isolated the target alkyne derivative **12c** in 75% yield. These last conditions applied to OTf intermediates **4** and **5b** in presence of various terminal alkynes, yielded target compounds **11** and **13a-c** in satisfactory yields (> 70 %, see table 2) (Scheme 3).

Negishi cross coupling reactions represent an extremely versatile tool for the introduction of alkyl substituents. As reported by Knochel et al. [60] and in presence of SPhos (10.0 mol %) and $Pd(OAc)_2$ (5.0 mol %) it was possible to perform at room temperature, efficient cross coupling reaction between OTf coumarin **5a-b** and benzyl zinc reagent (see scheme 3, cpds **14** and **15).**

Lastly, subsequent reduction of alkynes **12a** and **13a** was performed by catalytic hydrogenation, leading respectively to cpds **16** and **17** as depicted in scheme 3.

All synthesized compounds had their chemical structures confirmed by ^{1}H and ^{13}C NMR and mass spectrometry, and all spectra data are available in supplementary material.

3.2. Biological evaluation

3.2.1. Effects of coumarin derivatives on cell viability

All the synthetic coumarins (**7**, **8a-f**, **9a-g**, **10**, **11**, **12 a-c**, **13a-c**, **14-17**) were first screened for their *in vitro* cytotoxic activity at a single concentration (12 µM) against NSCLC cell line (human lung adenocarcinoma A549) for 24 h, using the well-established 3-(4,5-dimethylthiazol-2-yl)-2,5-diphenyltetrazolium bromide (MTT) assay. The results of A549 cells viability are reported in Figure 1.

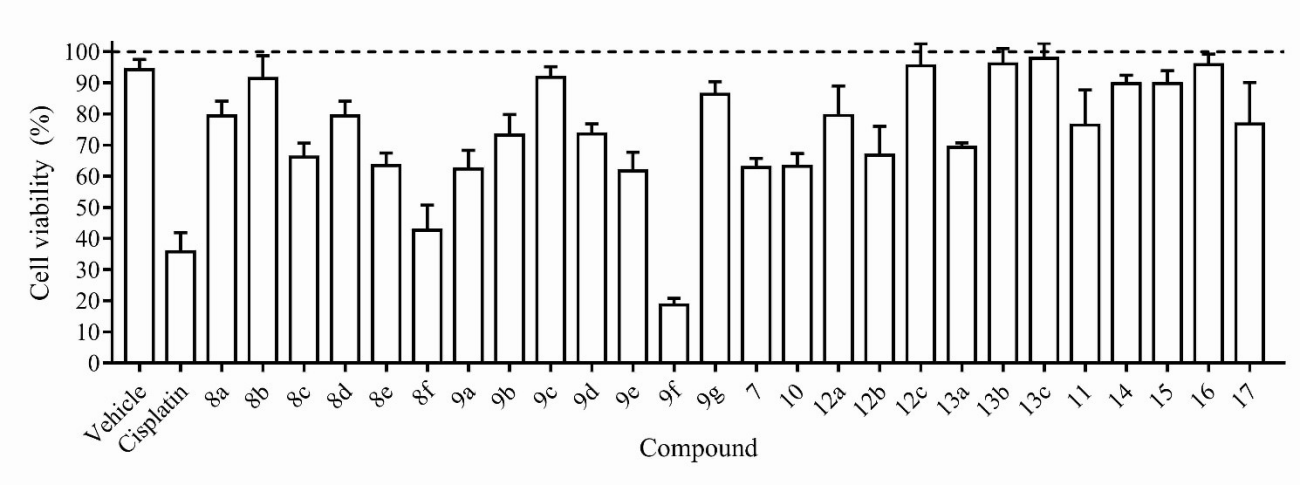

Figure 1. Effect of synthetic coumarin derivatives on cell viability. The viability of A549 cells was determined using the MTT assay after exposure at a single concentration (12 μM) of the compounds or cisplatin (2.6 μM) for 24 h. The percentage of inhibition was calculated considering the cells treated with medium (DMEM), considered as 100% of cell viability (dotted line). Bars represent the mean ± S.D. from three independent experiments.

The results showed that compounds **8b**, **9c**, **9g**, **12c**, **13b**, **13c**, **14**, **15**, and **16** showed little or no cytotoxicity. Compounds **7**, **8a**, **8c**, **8d**, **8e**, **9a**, **9b**, **9d**, **9e**, **10**, **11**, **12a-b**, **13a** and **17** showed a moderate cytotoxicity by inducing a reduction in cell viability within 80%–60%. And compounds **8f** and **9f**, which have in common the presence of a 3,4-dichloro-phenyl group ((3,4-Cl)-Ph), induced a strong cytotoxicity by decreasing the A549 cells viability to values below 50%.

Among these two compounds, **9f** was the most promising, reducing the A549 cells viability to less than 20%. Thus, this compound was selected and had its concentration that reduces the viable cell number by 50% (CC_{50}) determined against two cancer cell lines (human lung adenocarcinoma A549 and H2170 cell lines) and one non-cancer cell line (NIH-3T3), and showed CC_{50} values (mean ± S.D.) of 7.1 ± 0.8 μM, 3.3 ± 0.5 μM and 25.8 ± 1.7 μM against A549, H2170 and NHI-3T3 cells, respectively. Facing these results, we can notate that **9f** showed to be the most potent against cancer cells (A549 and H2170 cell lines) than against healthy cell (NIH-3T3 cell line).

These cytotoxicity results are better than those observed for the most cytotoxic coumarins from other studies against the A549 cells, such as: Umbelliprenin (IC_{50} = 52 ± 1.97 μM) [33]; 3-arylcoumarin derivative (8-(acetyloxy)-3-(4-methanesulfonyl phenyl)-2-oxo-2*H*-chromen-7-yl acetate) with IC_{50} = 24.2 μM [31]; and iodinated-4-aryloxymethylcoumarins (6-chloro- and 7-chloro-4-(4-iodo-phenoxymethyl)-chromen-2-one) with IC_{50} = 7.57 μM [35]; these latter bearing chlorine atoms in their structures, as observed in the most active compounds of the present study (coumarins **8f** and **9f**).

On the basis of cytotoxic effect, the concentration of 7 μM of **9f** was chosen for further to characterize the antitumor activity, by investigating their effects on the process of inhibition of the EMT-associated migratory ability and epithelial-to-mesenchymal transition (EMT) in IL-1β-stimulated A549 cells.

3.2.2. Effect of 9f on IL-1β-induced EMT in A549 cells

The EMT process is characterized by the phenotypic conversion of epithelial into mesenchymal cells that occurs with great frequency in fibrotic tissues, embryonic cells, and cancer. This transition increases the invasion capacity and the migratory potential of cells, which are characteristic of metastatic cancer, contributing additionally to the development of drug-resistance in cancer [61-66].

To determine whether compound **9f** acts as an inhibitory compound of EMT in epithelial cells, the morphological changes induced by IL1-β on A549 cells was observed. As shown in Figure 2A and 2B, the A549 cells maintained to culture medium (DMEM) or treated with compound **9f** exhibited, in a confluent monolayer, a cobblestone-like cell morphology, which is characteristic of epithelial cells. Cells treated with 1 ng/mL IL-1β exhibited an evident morphological change and acquired a spindle-like morphology with loss of cell-cell interactions that is characteristic features of mesenchymal cells (Figure 2C). A549 cells treated with **9f** exhibited an impairment in changes in its mesenchymal

253 characteristics induced by IL-1β (Figure 2D), suggesting that **9f** possess inhibitory effects on IL-1β-
254 induced F-actin reorganization.

255 To evaluate the effect of compound **9f** on actin cytoskeleton organization, A549 cells were IL-
256 1β-stimulated and evaluated by staining with FITC-labeled phalloidin. As presented in the Figure 2E
257 and 2F, the A549 cells maintained to culture medium (DMEM) or treated with **9f** exhibited an abundant
258 deposition of actin filament in the cortical region, which determines a cellular cobblestone-like
259 morphology, typical of epithelial cells. Stimulation with IL-1β induced a cytoskeleton reorganization,
260 leading to the activation of actin polymerization and the morphologic cell reorganization, which
261 indicate a differentiation from the epithelial to mesenchymal phenotype (Figure 2G). Treatment with
262 **9f** attenuated the changes in the actin cytoskeleton reorganization in A549 cells stimulated by IL-1β
263 (Figure 2H).

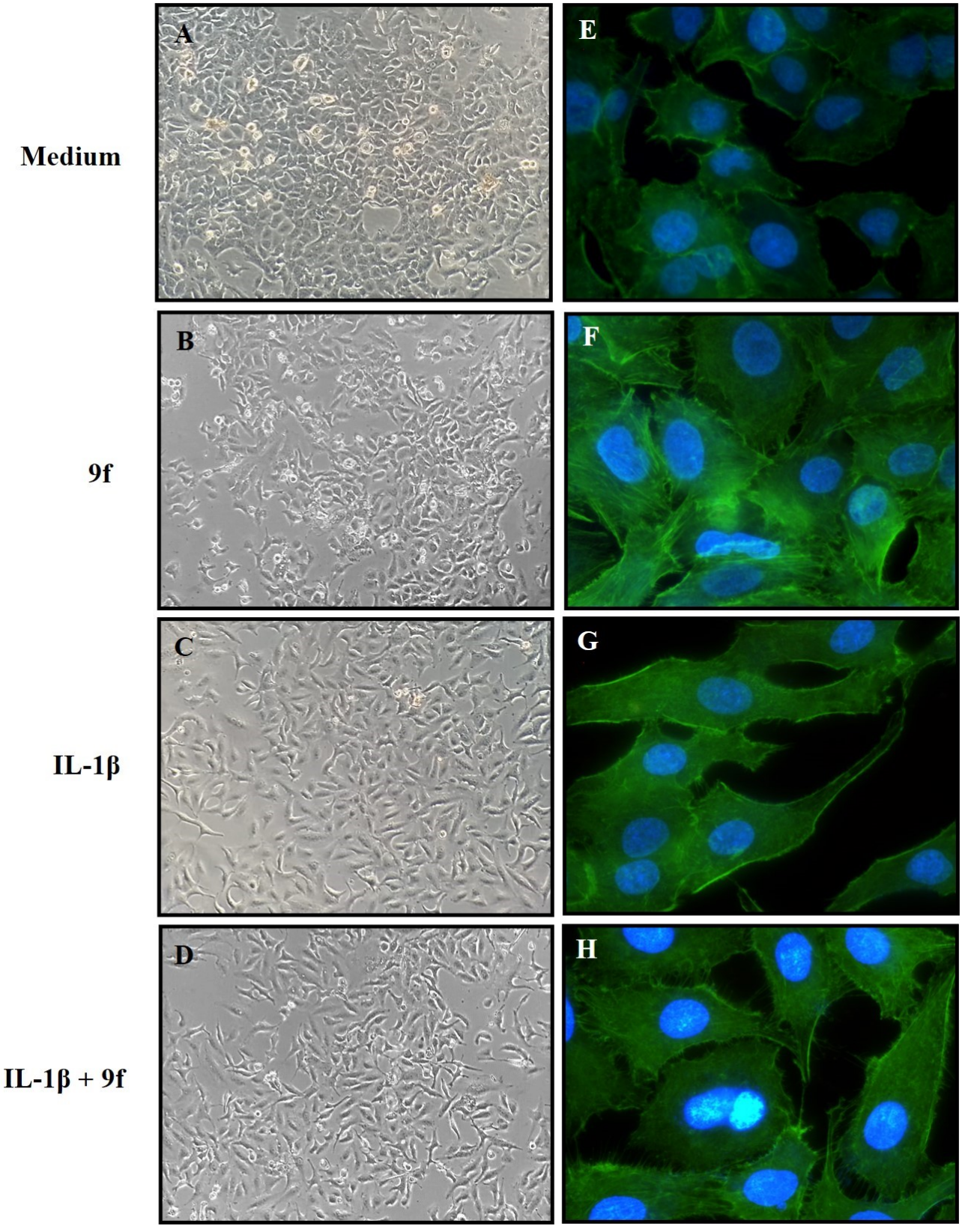

Figure 2. Compound **9f** inhibited IL-1β-induced EMT *in vitro*. A549 cells were treated with **9f** (7 μM) in the presence or absence of 1 ng/mL IL-1β. Cells were photographed using phase-contrast microscopy (A, B, C and D) or fluorescence microscopy (E, F, G e H). Cells were exposure to treatment with DMEM-medium (A and E), **9f** (B and F), IL-1β (C and G) or **9f** + IL-1β (D and H) for

24 h. Actin (green) was detected via immunofluorescence in formaldehyde-fixed cells with FITC-conjugated phalloidin (1:100). Nuclei were counterstained with DAPI. Magnification ×100 for phase-contrast microscope and ×400 for fluorescence microscope.

To corroborate whether this morphological transformation represents EMT, immunofluorescent staining was used to quantify the vimentin, a mesenchymal marker most commonly associated with EMT and involved in cancer progression [67].

As shown in Figure 3A, 24 h incubation with 1 ng/mL IL-1β increased significantly the expression of vimentin in A549 cells compared with those maintained DMEM medium (control). We found that treatment of cells with **9f** (7 μM) significantly diminished the expression of mesenchymal marker vimentin in IL-1β-stimulated A549 cells (Figure 3A), phenomenon confirmed by quantitative assessment by flow cytometer (Figure 3B-C). Treatment of cells with **9f** did not change levels of vimentin expression in unstimulated cells with IL-1β (Figure 3A-C). This result showed that **9f** treatment suppresses IL-1β-induced EMT in A549 cells through downregulating vimentin.

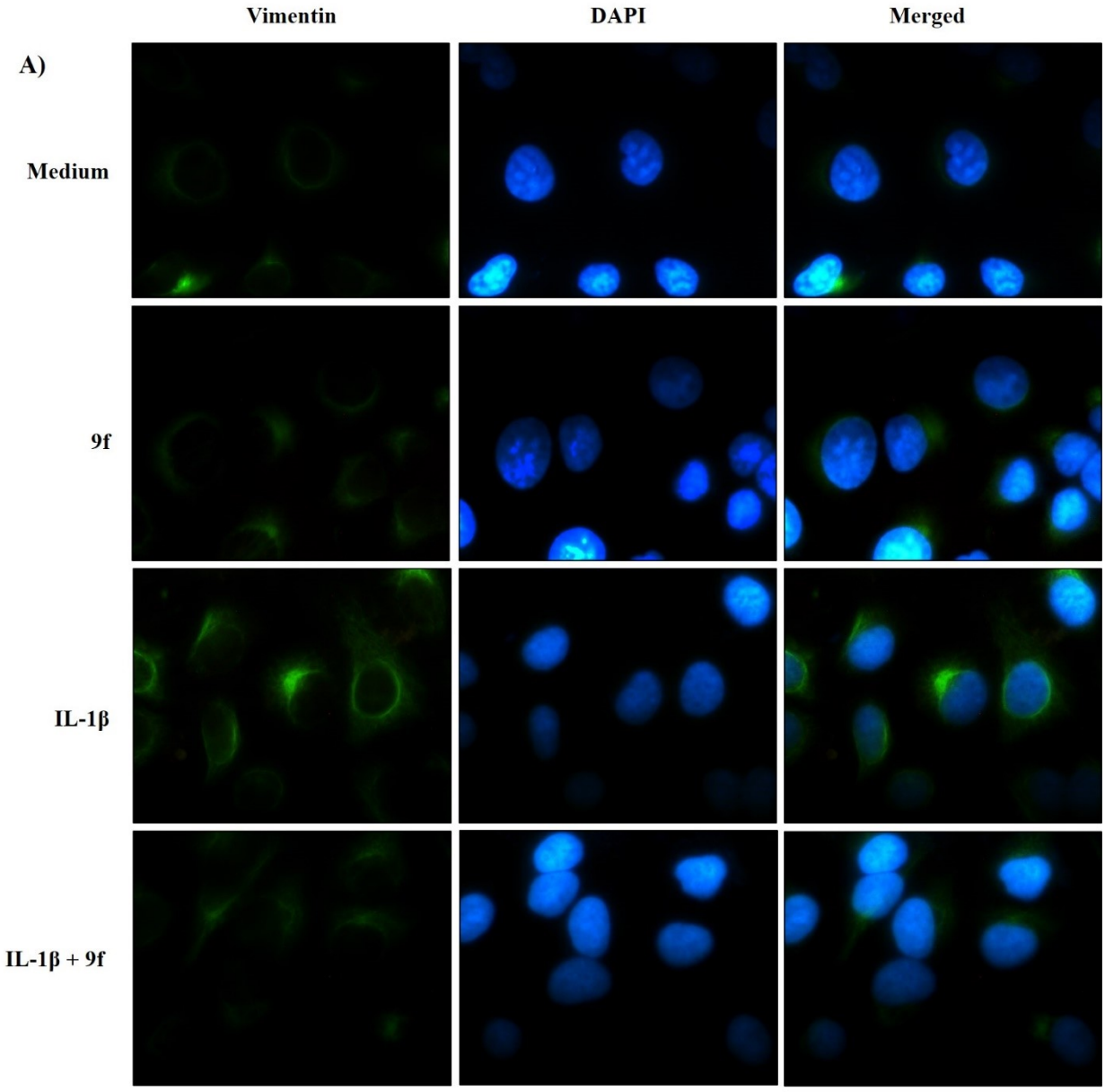
Vimentin
DAPI
Merged
A)
Medium
9f
IL-1β
IL-1β + 9f

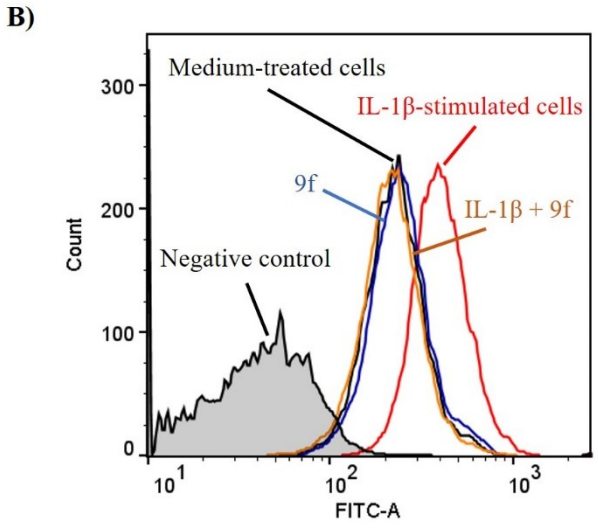
B)
Medium-treated cells
IL-1β-stimulated cells
9f
IL-1β + 9f
Negative control
Count
300
200
100
0
10^1
10^2
10^3
FITC-A

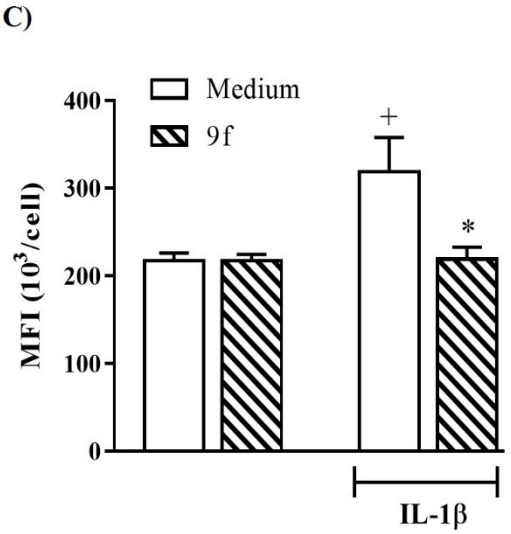
C)
Medium
9f
MFI (10^3/cell)
400
300
200
100
0
+
*
IL-1β

282

Figure 3. Compound **9f** downregulates the expression of mesenchymal cell marker vimentin in IL-1β-induced EMT. A549 cells were treated with compound **9f** (7 μM) in the presence or absence of 1 ng/mL IL-1β. The mesenchymal markers vimentin was detected by immunofluorescence. (A) Cells were exposure to treatment with DMEM-medium, **9f**, IL-1β or IL-1β+6f for 24 h. Vimentin (green) was detected via immunofluorescence in formaldehyde-fixed cells with FITC-conjugated antibody. Nuclei were counterstained with DAPI. Magnification ×400 for fluorescence microscope. (B) and (C) Flow cytometry analysis showing the reduced expression of vimentin in IL-1β-induced EMT under **9f** treatment. In graph in (C), bars represent mean ± S.D. from three independent experiments. (+) $P < 0.01$ compared with respective DMEM-treated cells and (*) $P < 0.01$ compared with IL-1β-stimulated cell medium-treated cells.

3.2.3. Effects of 9f on cells motility

Given the good results of **9f** in inhibiting the IL-1β-induced EMT in epithelial cells, was investigated whether **9f** could affected the EMT-associated migratory ability in A549 cells. For this, *in vitro* wound-healing assay was performed to evaluate as **9f** acts as anti-metastatic agent in A549 cells.

As shown in Figure 4A-B, IL-1β-treated cells exhibited an increased in wound closure within 24 h compared with those not treated with IL-1β (control). Treatment of cells with **9f** at 7 μM for 24 h significantly reduced migration of IL-1β-stimulated cells, phenomenon confirmed by qualitative assessment of the wound closure (Figure 4A-B).

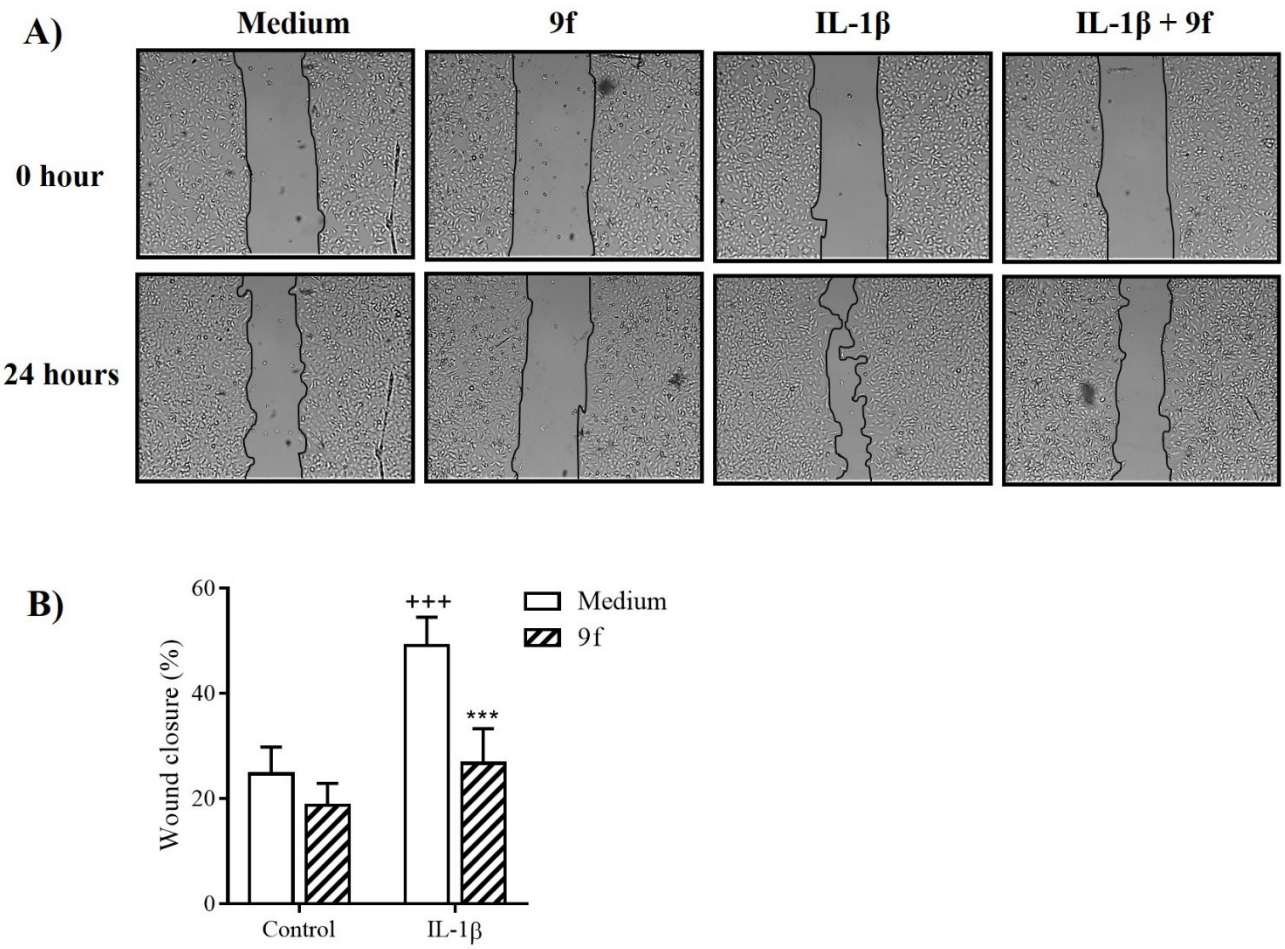

Figure 4. The effect of **9f** on the migration of A549 cells assayed by the wound healing assay. Cells were treated with **9f** at 7 μM, and images were captured to calculate the scratch closure. In A, representative photomicrography images showing the cell migration towards the cell-free area after treatment with DMEM (control) or **9f** and the after 24 h. In B, graph shows percentage of scratch covered was measured by quantifying the total distance the cells moved from the edge of the scratch towards the center of the scratch, using ImageJ software, followed by conversion to a percentage of the wound covered. Values represent mean ± S.D. from three independent experiments. (+++) $P < 0.001$ compared with respective DMEM-treated cells and (***) $P < 0.001$ compared with IL-1β-stimulated cell vehicle-treated cells.

In conclusion, twenty-six coumarin derivatives were synthesized through PCCCR and were evalauted for their anti-lung cancer properties against two non-small cell lung carcinoma (NSCLC) cell lines. Coumarins **8f** and **9f**, presenting a 3,4-dichloro-phenyl radical, inhibited *in vitro* the growth of both human lung adenocarcinoma cells in low micromolar concentration. Derivative **9f** regulate the epithelial-to-mesenchymal transition (EMT) suppressing the mesenchymal marker vimentin and

cancer cell migration in IL-1β-stimulated A549 cells. Taken together, our finding suggest that coumarin derivatives, especially compound **9f** may become a promising *hit* in the process of lung cancer drug discovery, especially in lung cancer promoted by non-small cell lung carcinoma (NSCLC) cell lines.

Declaration of competing interest

All the authors declare they have no conflict of interests for this work.

Acknowledgements

This work was supported by the Federal University of Alagoas (UFAL), State University of Paraiba (UEPB), by the Conselho Nacional de Desenvolvimento Científico e Tecnológico (CNPq) [grant numbers 308590/2017-1 and 306798/2020-4]. This study was financed in part by the Coordenação de Aperfeiçoamento de Pessoal de Nível Superior - Brasil (CAPES) – Finance Code 001 and by Paraiba State Research Foundation (FAPESQ) grant number 301724/2021-0 through concession of scholarship to R.S.A.A.

References

[1] S.N. Zafar, A.H. Siddiqui, R. Channa, S. Ahmed, A.A. Javed, A. Bafford, 2019. Estimating the Global Demand and Delivery of Cancer Surgery, World J. Surg. 43(9), 2203-2210. doi: 10.1007/s00268-019-05035-6.

[2] F. Bray, J. Ferlay, I. Soerjomataram, R.L. Siegel, L.A. Torres, A. Jemal, 2018. Global cancer statistics 2018: GLOBOCAN estimates of incidence and mortality worldwide for 36 cancers in 185 countries. CA Cancer J. Clin. 68, 394-424. doi: 10.3322/caac.21492.

[3] K. Ganesh, J. Massagué, 2021. Targeting metastatic câncer. Nat. Med. 27(1), 24-44. doi: 10.1038/s41591-020-01195-4.

[4] A.W. Lambert, D.R. Pattabiraman, R.A. Weinberg, 2017. Emerging Biological Principles of Metastasis. Cell. 168(4), 670-691. doi: 10.1016/j.cell.2016.11.037.

[5] S. Lamouille, J. Xu, R. Derynck, 2014. Molecular mechanisms of epithelial-mesenchymal transition. Nat. Rev. Mol. Cell. Biol. 15(3), 178-96. doi: 10.1038/nrm3758.

[6] W. Lu, Y. Kang, 2019. Epithelial-Mesenchymal Plasticity in Cancer Progression and Metastasis. Dev. Cell. 49(3), 361-374. doi: 10.1016/j.devcel.2019.04.010.

[7] A. Dongre, R.A. Weinberg, 2019. New insights into the mechanisms of epithelial-mesenchymal transition and implications for cancer. Nat. Rev. Mol. Cel.l Biol. 20(2), 69-84. doi: 10.1038/s41580-018-0080-4.

[8] G.W. Pearson, 2019. Control of Invasion by Epithelial-to-Mesenchymal Transition Programs during Metastasis. J. Clin. Med. 8(5), pii: E646. doi: 10.3390/jcm8050646.

[9] F. Marcucci, G. Stassi, R. De Maria, 2016. Epithelial-mesenchymal transition: a new target in anticancer drug discovery. Nat. Rev. Drug Discov. 15(5), 311-325. doi: 10.1038/nrd.2015.13.

[10] E.S. Cho, H.E. Kang, N.H. Kim, J.I. Yook, 2019. Therapeutic implications of cancer epithelial-mesenchymal transition (EMT). Arch. Pharm. Res. 42(1), 14-24. doi: 10.1007/s12272-018-01108-7.

[11] R.S.A. Araújo, F.J.B. Mendonça Junior. Coumarins: Synthetic Approaches and Pharmacological Importance, in: M.F.F.M. Diniz, L. Scotti, M.T. Scotti, M.F. Alves (Eds.), Natural Products and Drug Discovery: From Pharmacochemistry to Pharmacological Approaches, Editora UFPB, João Pessoa, 2018. pp. 245-274.

[12] S.-G. Zhang, C.-G. Liang, Y.-Q. Sun, P. Teng, J.-Q. Wang, W.-H. Zhang, 2019. Design, synthesis and antifungal activities of novel pyrrole- and pyrazole-substituted coumarin derivatives. Mol. Divers. 23, 915-925. doi :10.1007/s11030-019-09920-z.

[13] N.O. Mahmoodi, Z. Jalalifard, G.P. Fathanbari, 2020. Green synthesis of bis-coumarin derivatives using $Fe(SD)_3$ as a catalyst and investigation of their biological activities. J. Chin. Chem. Soc. 67, 172-182. doi: 10.1002/jccs.201800444.

[14] Y.K. Al-Majedy, H.H. Ibraheem, L.S. Jassim, A.A. Al-Amiery, 2019. Antioxidant activity of coumarine compounds, ANJS. 22, 1-8. doi: 10.22401/ANJS.22.1.01.

[15] T. Wang, T. Peng, X. Wen, G. Wang, S. Liu, Y. Sun, S. Zhang, L. Wang, 2020. Design, synthesis and evaluation of 3-substituted coumarin derivatives as anti-inflammatory agents, Chem. Pharm. Bull (Tokyo). c19-01085. doi: 10.1248/cpb.c19-01085.

[16] T.K. Mohamed, R.Z. Batran, S.A. Elseginy, M.M. Ali, A.E. Mahmoud, 2019. Synthesis, anticancer effect and molecular modeling of new thiazolylpyrazolyl coumarin derivatives targeting VEGFR-2 kinase and inducing cell cycle arrest and apoptosis, Bioorg. Chem. 85, 253-273. doi: 10.1016/j.bioorg.2018.12.040.

[17] K. Kasperkiewicz, M.B. Ponczek, J. Owczarek, P. Guga, E. Budzisz, 2020. Antagonists of vitamin K – Popular coumarin drugs and new synthetic and natural coumarin derivatives, Molecules. 25, 1465-1488. doi: 10.3390/molecules25061465.

[18] R.D. Thornes, L. Daly, G. Lynch, B. Breslin, H. Browne, H.Y. Browne, T. Corrigan, P. Daly, G. Edwards, E. Gaffney, J. Henley, T. Healy, F. Keane, F. Lennon, N. McMurray, S. O'Loughlin, M. Shine, A. Tanner, 1994. Treatment with coumarin to prevent or delay recurrence of malignant melanoma. J. Cancer. Res. Clin. Oncol. 120(Suppl), S32-34. doi: 10.1007/bf01377122.

[19] M.E. Marshall, J.L. Mohler, K. Edmonds, B. Williams, K. Butler, M. Ryles, L. Weiss, D. Urban, A. Bueschen, M. Markiewicz, G. Cloud, 11994. An updated review of the clinical development of coumarin (1,2-benzopyrone) and 7-hydroxycoumarin. J. Cancer Res. Clin. Oncol. 120(Suppl), S39-42. doi: 10.1007/bf01377124.

[20] E. von Angerer, M. Kager, A. Maucher, 1994. Anti-tumour activity of coumarin in prostate and mammary cancer models. J. Cancer Res. Clin. Oncol. 120(Suppl), S14-16. doi: 10.1007/bf01377116.

[21] J.S. Lopez-Gonzalez, H. Prado-Garcia, D. Aguilar-Cazares, J.A. Molina-Guarneros, J. Morales-Fuentes, J.J. Mandoki, 2004. Apoptosis and cell cycle disturbances induced by coumarin and 7-hydroxycoumarin on human lung carcinoma cell lines. Lung Cancer. 43(3), 275-283. doi: https://doi.org/10.1016/j.lungcan.2003.09.005.

[22] S. Emami, S. Dadashpour, 2015. Current developments of coumarin-based anti-cancer agents in medicinal chemistry. Eur. J. Med. Chem. 102, 611-630. doi: 10.1016/j.ejmech.2015.08.033.

[23] J. Dandriyal, R. Singla, M. Kumar, V. Jaitak, 2016. Recent developments of C-4 substituted coumarin derivatives as anticancer agents. Eur. J. Med. Chem. 119, 141-168. doi: 10.1016/j.ejmech.2016.03.087.

[24] A. Thakur, R. Singla, V. Jaitak, 2015. Coumarins as anticancer agents: a review on synthetic strategies, mechanism of action and SAR studies. Eur .J. Med. Chem. 101, 476-495. doi: 10.1016/j.ejmech.2015.07.010.

[25] L. Zhang, Z. Xu, 2019. Coumarin-containing hybrids and their anticancer activities. Eur. J. Med. Chem. 181, 111587. doi: 10.1016/j.ejmech.2019.111587.

[26] J. Klenkar, M. Molnar, 2015. Natural and synthetic coumarins as potential anticancer agents. J. Chem. Pharm. Res. 7(7), 1223-1238.

[27] S. Kawaii, Y. Tomono, K. Ogawa, M. Sugiura, M. Yano, Y. Yoshizawa, 2001. The anti-proliferative effect of coumarins on several cancer cell lines. Anticancer Res. 21, 917-923.

[28] M. Kumar, R. Singla, J. Dandriyal, V. Jaitak, 2018. Coumarin Derivatives as Anticancer Agents for Lung Cancer Therapy: A Review. Anticancer Agents Med. Chem. 8(7), 964-984. doi: 10.2174/1871520618666171229185926.

[29] K.G. Weng, Y.L. Yuan, 2017. Synthesis and evaluation of coumarin derivatives against human lung cancer cell lines. Braz. J. Med. Biol. Res. 50(11), e6455. doi: 10.1590/1414-431X20176455.

[30] Y. Wang, C.F. Li, L.M. Pan, Z.L. Gao, 2013. 7,8-Dihydroxycoumarin inhibits A549 human lung adenocarcinoma cell proliferation by inducing apoptosis via suppression of Akt/NF-κB signaling. Exp. Ther. Med, 5(6), 1770-1774. doi: 10.3892/etm.2013.1054.

[31] M.A. Musa, M.Y. Joseph, L.M. Latinwo, V. Badisa, J.S. Cooperwood, 2015. In vitro evaluation of 3-arylcoumarin derivatives in A549 cell line. Anticancer Res. 35(2), 653-659.

[32] M.A. Musa, L.D.V. Badisa, L.M. Latinwo, T.A. Patterson, A.M. Owens, 2012. Coumarin-based Benzopyranone Derivatives Induced Apoptosis in Human Lung (A549) Cancer Cells. Anticancer Res. 32, 4271-4276.

[33] N. Khaghanzadeh, Z. Mojtahedi, M. Ramezani, N. Erfani, A. Ghaderi, 2012. Umbelliprenin is cytotoxic against QU-DB large cell lung cancer cell line but anti-proliferative against A549 adenocarcinoma cells. DARU J. Pharm. Sci. 20(1), 69-74.

[34] X. Xiaoman, Y. Zhang, D. Qu, T. Jiang, S. Li, 2011. Osthole induces G2/M arrest and apoptosis in lung cancer A549 cells by modulating PI3K/Akt pathway. *J. Exp. Clin. Cancer Res.* 30(33), 1-7.

[35] M. Basanagouda, V.B. Jambagi, N.N. Barigidad, S.S. Laxmeshwar, V. Devaru, Narayanachar, 2014. Synthesis, structure-activity relationship of iodinated-4-aryloxymethyl-coumarins as potential anti-cancer and anti-mycobacterial agents. Eur. J. Med. Chem. 74, 225-233. doi: 10.1016/j.ejmech.2013.12.061.

[36] F. Belluti, G. Fontana, L. Dal Bo, N. Carenini, C. Giommarelli, F. Zunino, 2010. Design, synthesis and anticancer activities of stilbene-coumarin hybrid compounds: Identification of novel proapoptotic agents. Bioorg. Med. Chem., 2010, 18, 3543- 3550. doi: 10.1016/j.bmc.2010.03.069.

[37] Y. Chen, H.R. Liu, H.S. Liu, M. Cheng, P. Xia, K. Qian, P.C. Wu, C.Y. Lai, Y. Xia, Z.Y. Yang, S.L. Morris-Natschke, K.H. Lee, 2012. Antitumor agents 292. Design, synthesis and pharmacological study of S- and O-substituted 7-mercapto- or hydroxy-coumarins and chromones as potent cytotoxic agents. Eur. J. Med. Chem. 49, 74-85. doi: 10.1016/j.ejmech.2011.12.025.

[38] F. Borges, F. Roleira, N. Milhazes, L. Santana, E. Uriarte, 2005. Simple coumarins and analogues in medicinal chemistry: Occurrence, synthesis and biological activity, Curr. Med. Chem. 12, 887-916. doi: 10.2174/0929867053507315.

[39] B.G. Lake, 1999. Coumarin metabolism, toxicity and carcinogenicity: relevance for human risk assessment. Food Chem. Toxicol. 37, 423-453. doi: 10.1016/s0278-6915(99)00010-1.

[40] T.-C. Wang, Y.-L. Chen, C.-C. Tzeng, S.-S. Liou, W.-F. Tzeng, Y.-L. Chang, C.-M. Teng, 1998. α-Methylidene-γ-butyrolactones: Synthesis and evaluation of quinolin-2(1*H*)-one derivatives, Helv. Chim. Acta. 81, 1038-1047. doi: 10.1002/hlca.19980810517.

[41] M. Spadafora, V.Y. Postupalenko, V.V. Shvadchak, A.S. Klymchenko, Y. Mély, A. Burger, R. Benhida, 2009. Efficient synthesis of ratiometric fluorescent nucleosides featuring 3-hydroxychromone nucleobases, Tetrahedron. 65, 7809-7816. doi: 10.1016/j.tet.2009.07.021.

[42] L. Plougastel, M.R. Pattanayak, M. Riomet, S. Bregant, A. Sallustrau, M. Nothisen, A. Wagner, D. Audisio, F. Taran, 2019. Sydnone-based turn-on fluorogenic probes for no-wash protein labeling and in-cell imaging, Chem. Commun. 55, 4582-4585. doi: 10.1039/C9CC01458F.

[43] A. Kumar, M.L.N. Rao, 2018. Pot-economic synthesis of diarylpyrazoles and pyrimidines involving Pd-catalyzed cross-coupling of 3-trifloxychromone and triarylbismuth, J. Chem. Sci. 130, 165-175. doi: 10.1007/s12039-018-1565-6.

[44] Š. Starčević, P. Brožič, S. Turk, J. Cesar, T.L. Rižner, S. Gobec, 2011. Synthesis and biological evaluation of (6- and 7-phenyl) coumarin derivatives as selective nonsteroidal inhibitors of 17*β*-hydroxysteroid dehydrogenase type 1, J. Med. Chem. 54, 248-261. doi: 10.1021/jm101104z.

[45] Y. Yamaguchi, N. Nishizono, D. Kobayashi, T. Yoshimura, K. Wada, K. Oda, 2017. Evaluation of synthesized coumarin derivatives on aromatase inhibitory activity, Bioorg. Med. Chem. Lett. 27, 2645-2649. doi: 10.1016/j.bmcl.2017.01.062.

[46] S.G. Das, B. Srinivasan, D.L. Hermanson, N.P. Bleeker, J.M. Doshi, R. Tang, W.T. Beck, C. Xing, 2011. Structure-activity relationship and molecular mechanisms of ethyl 2-amino-6-(3,5-

dimethoxyphenyl)-4-(2-ethoxy-2-oxoethyl)-4*H*-chromene-3-carboxylate (CXL017) and its analogues, J. Med. Chem. 54, 5937-5948. doi: 10.1021/jm200764t.

[47] G. Aridoss, B. Zhou, D.L. Hermanson, N.P. Bleeker, C. Xing, 2012. Structure-activity relationship (SAR) study of ethyl 2-amino-6-(3,5-dimethoxyphenyl)-4-(2-ethoxy-2-oxoethyl)-4*H*-chromene-3-carboxylated (CXL017) and the potential of the lead against multidrug resistance in cancer treatment, J. Med. Chem. 55, 5566-5581. doi: 10.1021/jm300515q.

[48] L. Peng, J. Jiang, C. Peng, N. Dai, Z. Tang, Y. Jiao, J. Chen, X. Xu, 2017. Synthesis of Unsymmetrical Aromatic Acetylenes by Diphenyl Chlorophosphate-Promoted Condensation Reaction of Aromatic Aldehydes and Sulfones, Chin. J. Org. Chem. 37, 3013-3018. doi: 10.6023/cjoc201704053.

[49] A. Elangovan, J.-H. Lin, S.-W. Yang, H.-Y. Hsu, T.-I. Ho, 2004. Synthesis and electrogenerated chemiluminescence of donor-substituted phenylethylcoumarins, J. Org. Chem. 69, 8086-8092. doi: 10.1021/jo0493424.

[50] C. Yadav, V. K. Maka, S. Payra, J. N. Moorthy, 2020. Multifunctional porous organic polymers (POPs): Inverse adsorption of hydrogen over nitrogen, stabilization of Pd(0) nanoparticles, and catalytic cross-coupling reactions and reductions. J. Catalys. 284, 61-71. doi: 10.1016/j.jcat.2020.02.002.

[51] R.I. Geran, N.H. Greenberg, M.M. MacDonald, A. Schumacher, B.J. Abbott, 1972. Protocols for screening chemical agents and natural products against animal tumors and other biological systems, Cancer Chemoth. Rep. 3, 17–27. doi:

[52] J. Wang, L. Bao, B. Yu, Z. Liu, W. Han, C. Deng, C. Guo, 2015. Interleukin-1β Promotes Epithelial-Derived Alveolar Elastogenesis via αvβ6 Integrin-Dependent TGF-β Activation. Cell. Physiol. Biochem. 36(6), 2198-2216. doi: 10.1159/000430185.

[53] S.H. Cardoso, C.R. de Oliveira, A.S. Guimarães, J. Nascimento, J. de Oliveira Dos Santos Carmo, J.N. de Souza Ferro, A.C. de Carvalho Correia, E. Barreto, 2018. Synthesis of newly functionalized 1,4-naphthoquinone derivatives and their effects on wound healing in alloxan-induced diabetic mice. Chem. Biol. Interact. 291, 55-64. doi: 10.1016/j.cbi.2018.06.007.

[54] A.F. Littke, G.C. Fu, 2002. Palladium-catalyzed coupling reactions of aryl chlorides, Angew. Chem. Int. Ed. 41, 4176-4211. doi: 10.1002/1521-3773(20021115)41:22<4176::AID-ANIE4176>3.0.CO;2-U.

[55] A. Mori, M.S.M. Ahmed, A. Sekiguchi, K. Masui, T. Koike, 2002. Sonogashira coupling with aqueous ammonia, Chem. Lett. 31, 756-757. doi: 10.1246/cl.2002.756.

[56] F. Bellina, A. Carpita, R. Rossi, 2004. Palladium catalysts for the Suzuki cross-coupling reaction: An overview of recent advances, Synthesis. 2004, 2419-2440. doi: 10.1055/s-2004-831223.

[57] Z.-Y. Tang, Q.-S. Hu, 2004. Room temperature nickel(0)-catalyzed suzuki-miyaura cross-couplings of activated alkenyl tosylates: Efficient synthesis of 4-substituted coumarins and 4-substituted 2-(5*H*)-furanones, Adv. Synth. Catal. 346, 1635-1637. doi: 10.1002/adsc.200404150.

[58] D. Završnik, S. Muratović, D. Makuc, J. Plavec, M. Cetina, A. Nagl, E. De Clercq, J. Balzarini, M. Mintas, 2011. Benzylidene-bis-(4-hydroxycoumarin) and benzopyrano-coumarin derivatives: Synthesis, $^{1}H/^{13}C$-NMR conformational and X-ray crystal structure studies and *in vitro* antiviral activity evaluations, Molecules. 16, 6023-6040. doi: 10.3390/molecules16076023.

[59] D.F. Chorley, D.P. Furkert, M.A. Brimble, 2016. Synthesis of the spiroketal core of the pinnatifinoside family of natural products, Eur. J. Org. Chem. 2016, 314-319. doi: 10.1002/ejoc.201501225.

[60] G. Manolikakes, Z. Dong, H. Mayr, J. Li, P. Knochel, 2009. Negishi Cross-Coupling Compatible with Unprotected Amide Functions, Chem. Eur. J. 15(6), 1324-1328. doi: 10.1002/chem.200802349.

[61] N. Gavert, A. Ben-Ze´ev, 2008. Epithelial-mesenchymal transition and the invasive potential of tumors, Trends Mol. Med. 14, 199–209. doi: 10.1016/j.molmed.2008.03.004.

[62] F. Bruzzese, A. Leone, M. Rocco, C. Carbone, G. Piro, M. Caraglia, E. Di Gennaro, A. Budillon, 2011. HDAC inhibitor vorinostat enhances the antitumor effect of gefitinib in squamous cell carcinoma of head and neck by modulating ErbB receptor expression and reverting EMT, J. Cell Physiol. 226, 2378–2390. doi: 10.1002/jcp.22574.

[63] S. Valastyan, R.A. Weinberg, 2011. Tumor metastasis: molecular insights and evolving paradigms, Cell 147, 275–292. doi: 10.1016/j.cell.2011.09.024.

[64] A.M. Arias, 2001. Epithelial mesenchymal interactions in cancer and development, Cell 105, 425–431. doi: 10.1016/s0092-8674(01)00365-8.

[65] R. Kalluri, R.A. Weinberg, 2009. The basics of epithelial-mesenchymal transition. J. Clin. Invest. 119, 1420–1428. doi: 10.1172/JCI39104.

[66] L. Yan, H.H. Yu, Y.S. Liu, Y.S. Wang, W.H. Zhao, 2019. Esculetin enhances the inhibitory effect of 5-Fluorouracil on the proliferation, migration and epithelial-mesenchymal transition of colorectal cancer. Cancer Biomark. 24(2), 231-240. doi: 10.3233/CBM-181764.

[67] Y.N. Jiang, X.Y. Ni, H.Q. Yan, L. Shi, N.N. Lu, Y.N. Wang, Q. Li, F.G. Gao, 2019. Interleukin 6-triggered ataxia-telangiectasia mutated kinase activation facilitates epithelial-to-mesenchymal transition in lung cancer by upregulating vimentin expression. Exp. Cell. Res. 381(2), 165-171. doi: 10.1016/j.yexcr.2019.05.011.

Highlights

- Coumarin derivatives were synthesized through palladium-catalyzed cross-coupling reactions.
- Compound **9f** is high cytotoxicity against NSCLC cell lines (A549 and H2170).
- **9f** reverses EMT by attenuation of changes in the actin cytoskeleton reorganization.
- **9f** suppresses IL-1β-induced EMT in A549 cells through downregulating vimentin.
- Wound-healing assay confirmed that **9f** reduces cancer cell migration of IL-1β-stimulated cells.